CORRECT SIZING OF THE REFLECTORS IN THE ULTRASONIC INSPECTION OF THE FORGING TITANIUM ALLOY

TH.TRANCĂ, I. RADU, R. ZEMAN

TITANIUM'S PROPERTIES

Exceptional Strength-to-Weight Ratio
Low Density
Excellent, Natural Corrosion Resistance
Superior Erosion Resistance
Erosion/Corrosion Resistance to Seawater
High Operational . Termal Conductivity
Low Modulus of Elasticity
Low Coeffi cient of Expansion
Non-Magnetic
Biocompatible
Extremely Short Half-Life
Dramatic Appearance
Compatibility with Graphite Composites
Environmentally Friendly

GLOBAL APPLICATIONS FOR TITANIUM . . .

Aerospace: Titanium's First and Foremost Market

Jet Engines
Airframes
Tick-Section Titanium

Non-Aerospace Global Industrial Applications

Heat Exchangers
Power Generation
Chemical Processing
Off shore Oil and Gas
Downhole Oil and Gas
Petroleum Processing
Marine Applications
Desalination
Armor/Armament
Metal Recovery and Finishing
Chlor-Alkali Processing
Pulp and Paper
Flue Gas Desulphurization
Food and Pharmaceutical
Nuclear Waste Storage
High Technology
Metal Matrix Composites
Titanium Aluminides
Ferrotitanium
Other Industrial Applications
Commercial and Consumer Goods
Healthcare
Architecture/Construction
Automotive

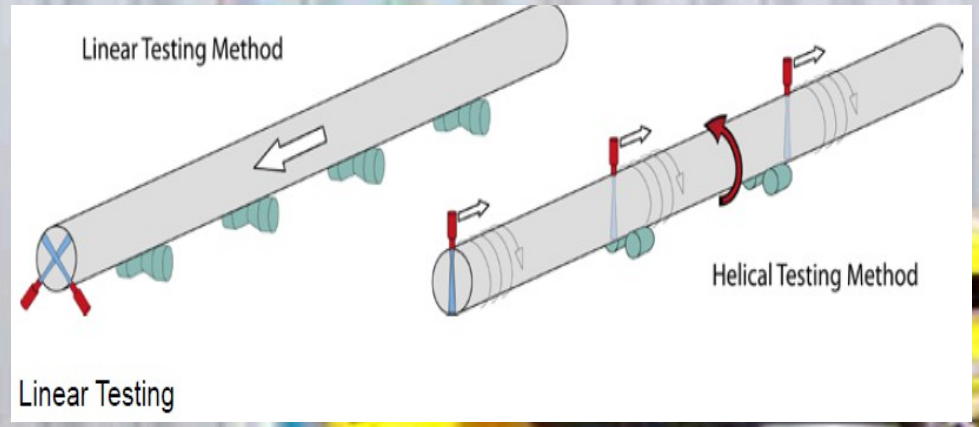

The ultrasonic inspection of the Titanium forgings billets is performed using Linear Testing or Helical Testing

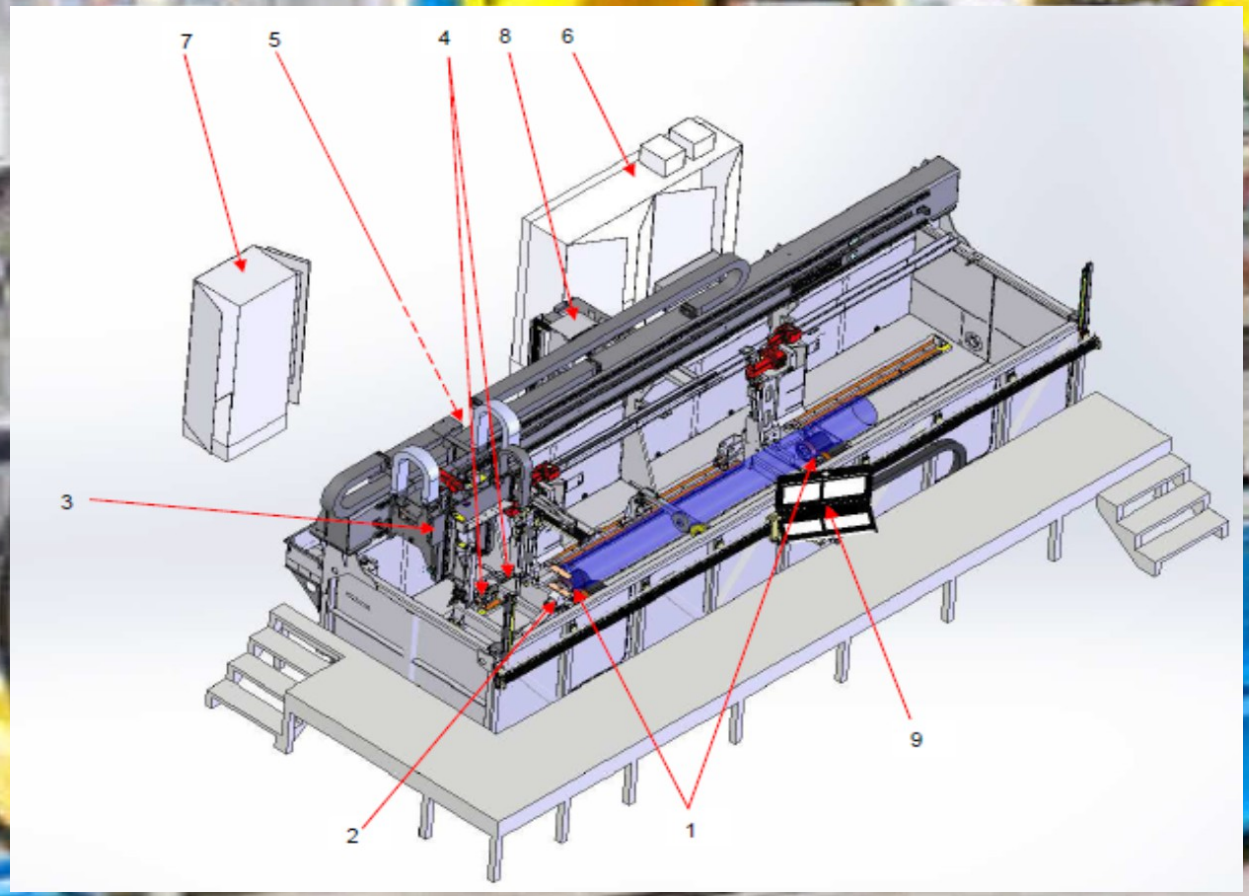

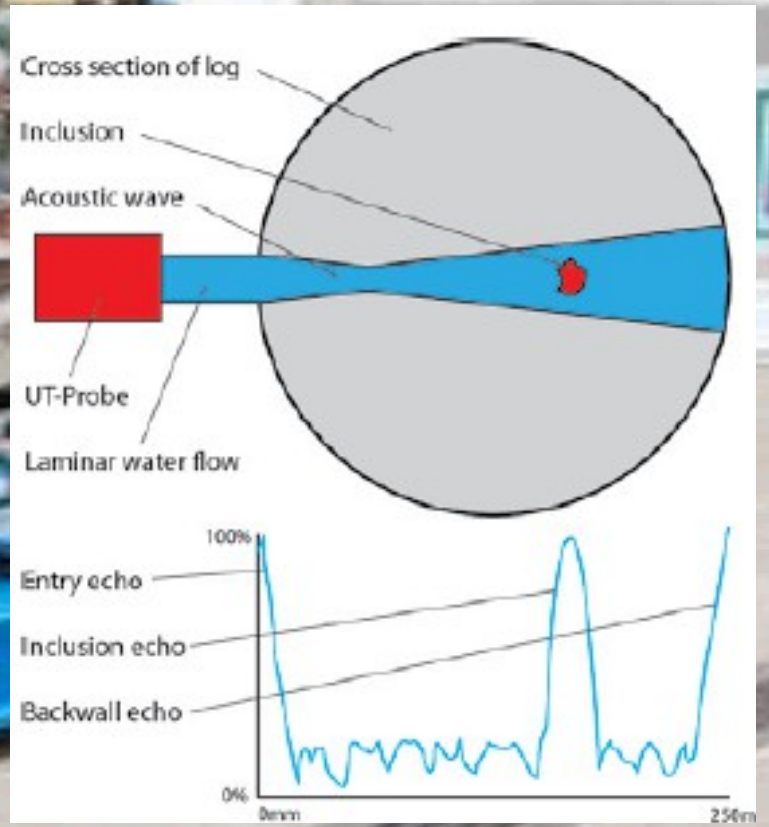

AUTOMATED ULTRASONIC TESTING

- Helical Testing -

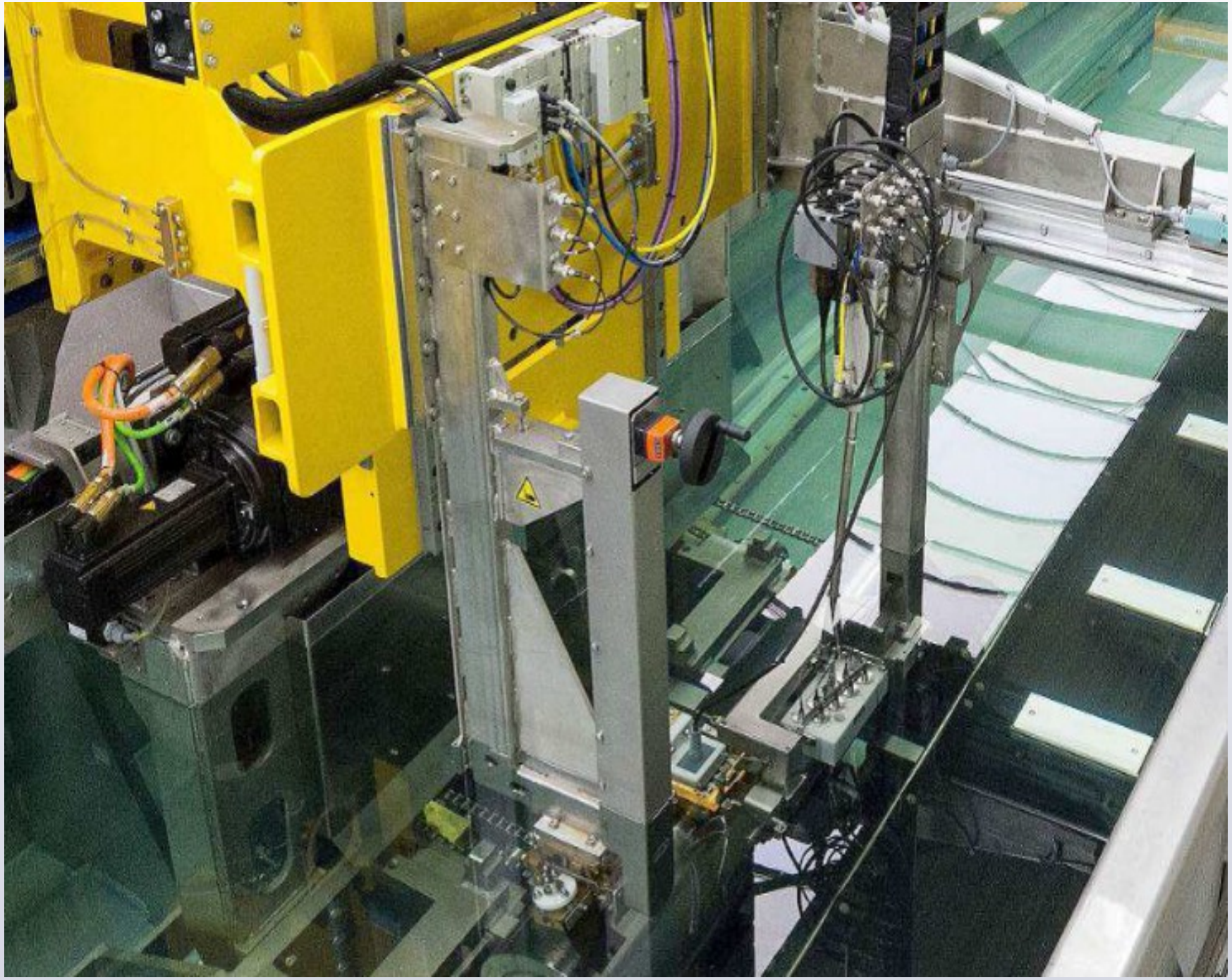

Sensitivity calibration setting using FBH

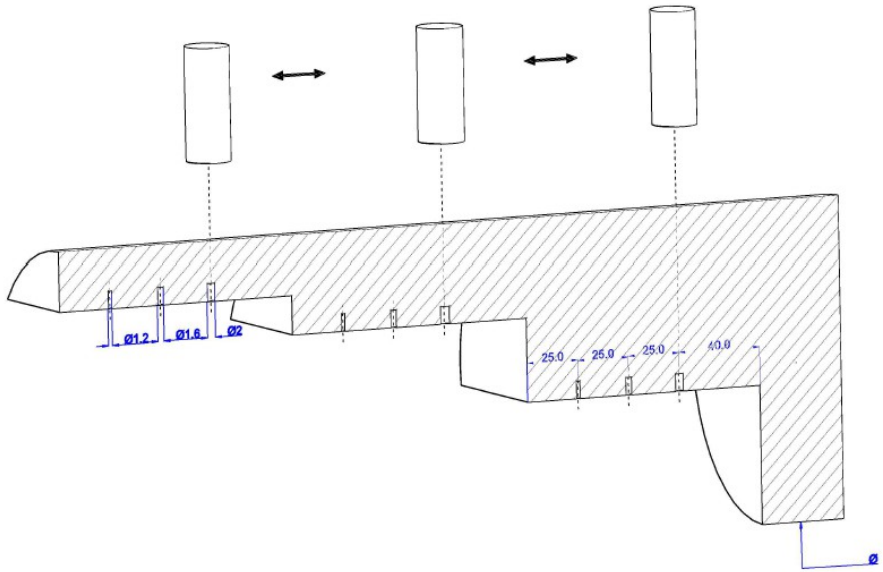

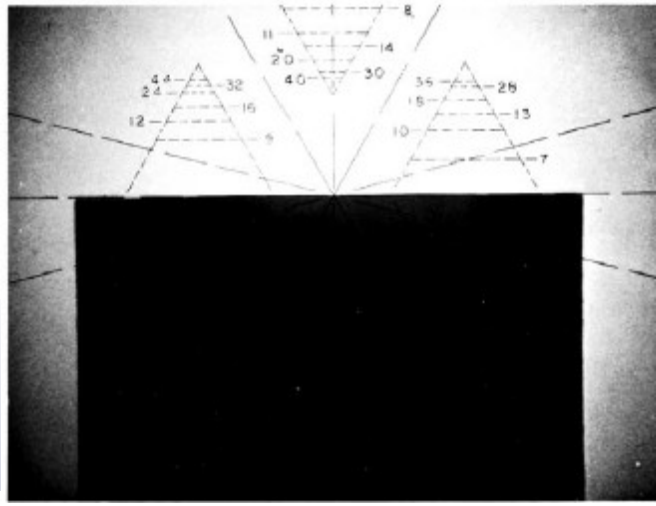

Flat Bottom Hole-- replica profile

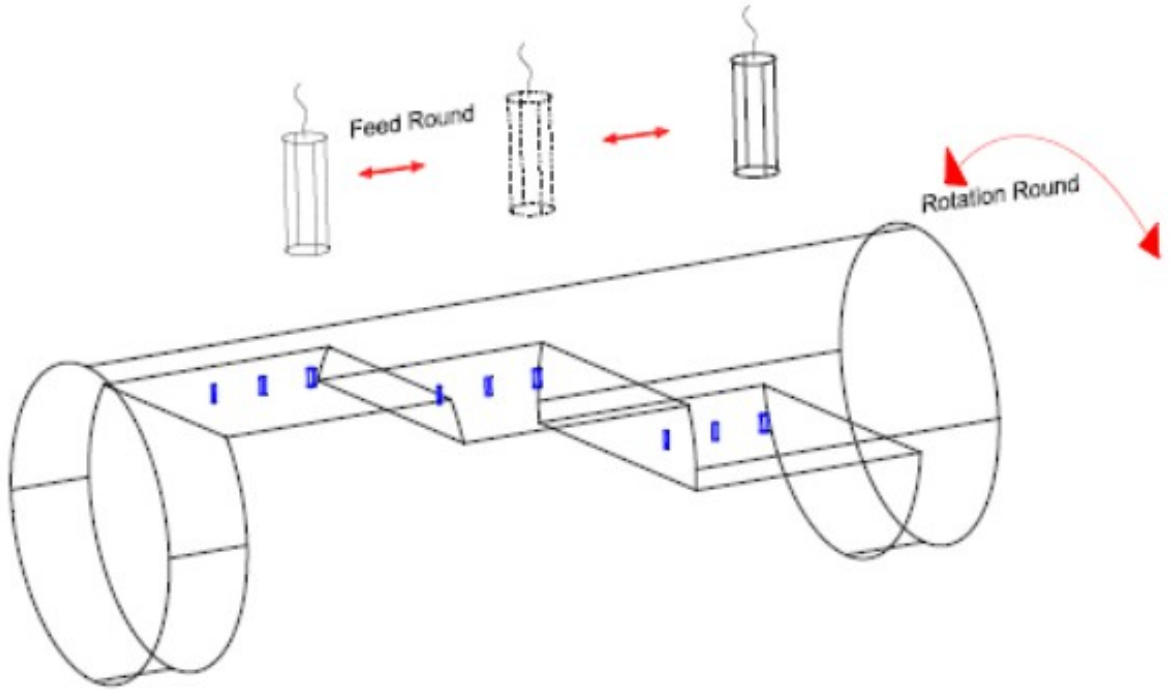

DISAGREEMENT WITH AREA AMPLITUDE RELATIONSHIP of Kirchhoff

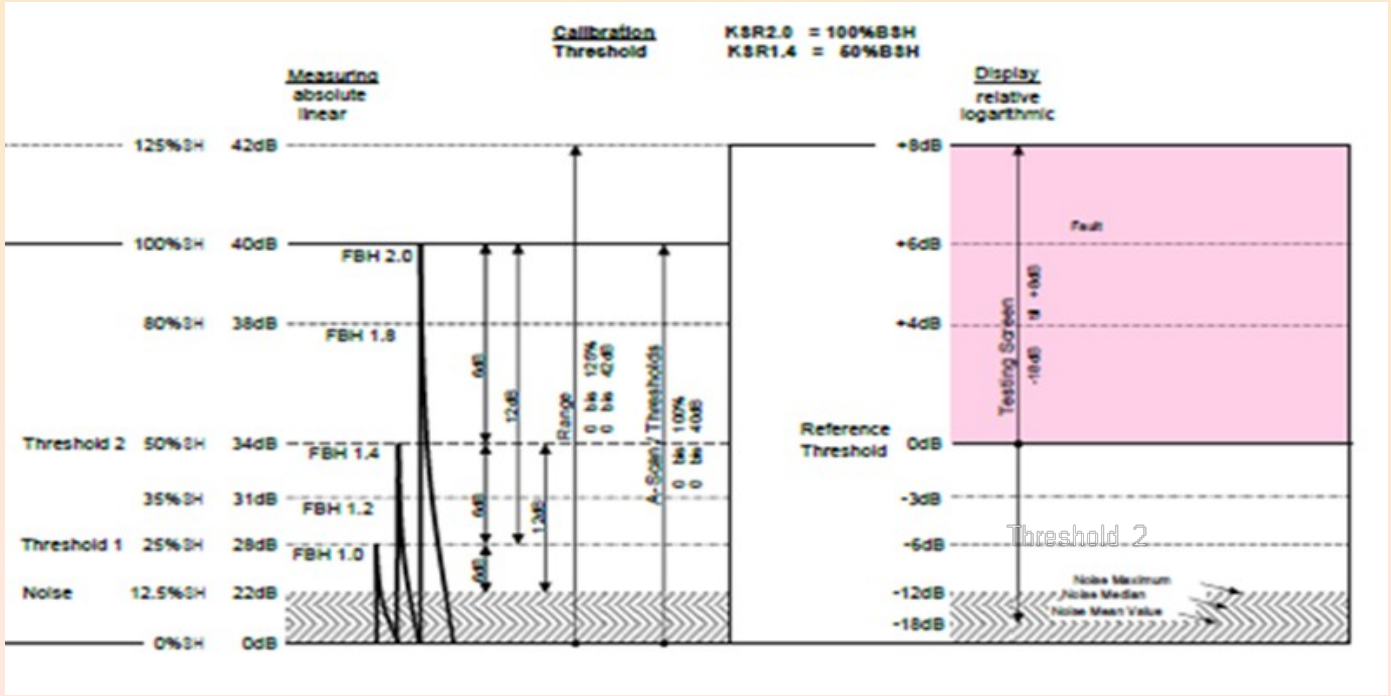

- General formula predicts an output voltage in direct proportion to the area of the FBH, i.e., the area amplitude relationship (Kirchhoff Aproximation)

$$\frac{V_f}{V_o} = \frac{SA}{\lambda^2 T^2} e^{-2T\delta}$$

Vf = the maximum amplitude of the echo from the FBH
Vo = the maximum possible signal amplitude if all energy is returned to the receiver
T = the distance along the beam axis to the target
A = the area of the probe
S = the area of the FBH
λ = the wavelength of ultrasound (nominal)
δ = the attenuation coefficient

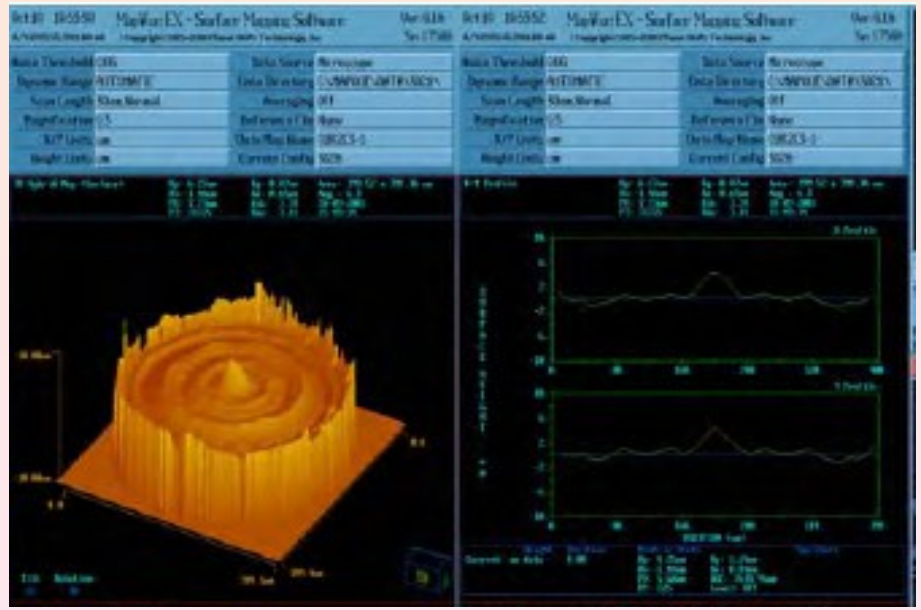

Example of Laser Profilometer Measurements

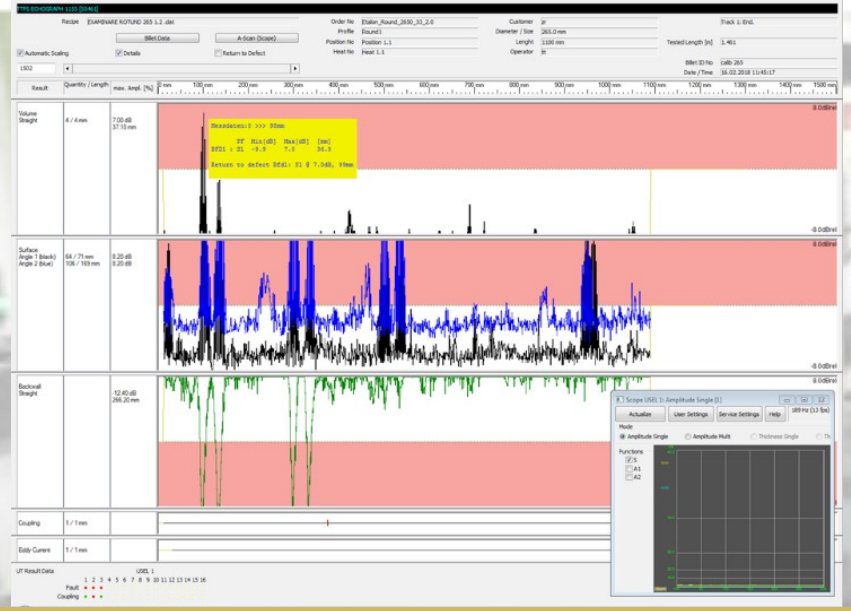

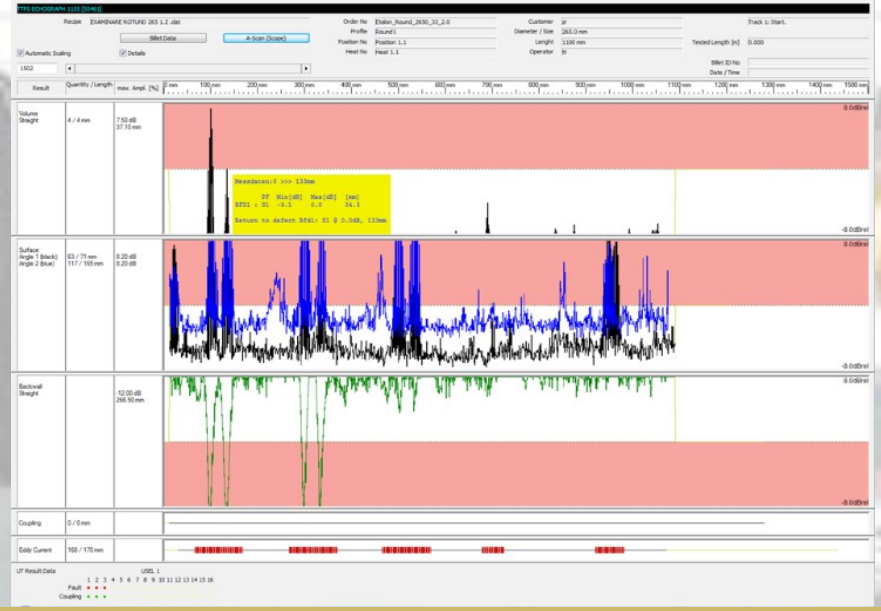

The difference between the signals of Φ 2.0 mm FBH and Φ 1.2 mm FBH is measured 7.5 dB instead of 8.87 dB, the theoretical value (Φ 265.0 mm reference block).

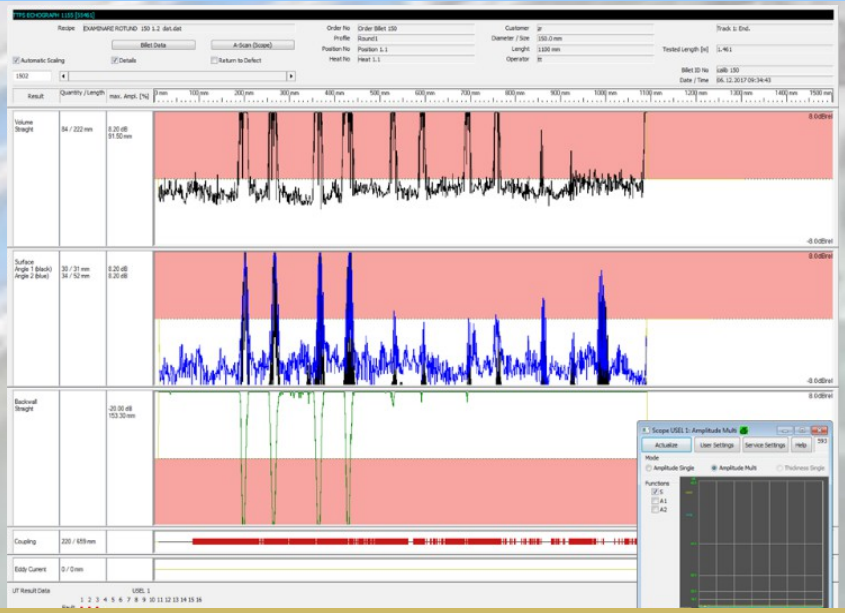

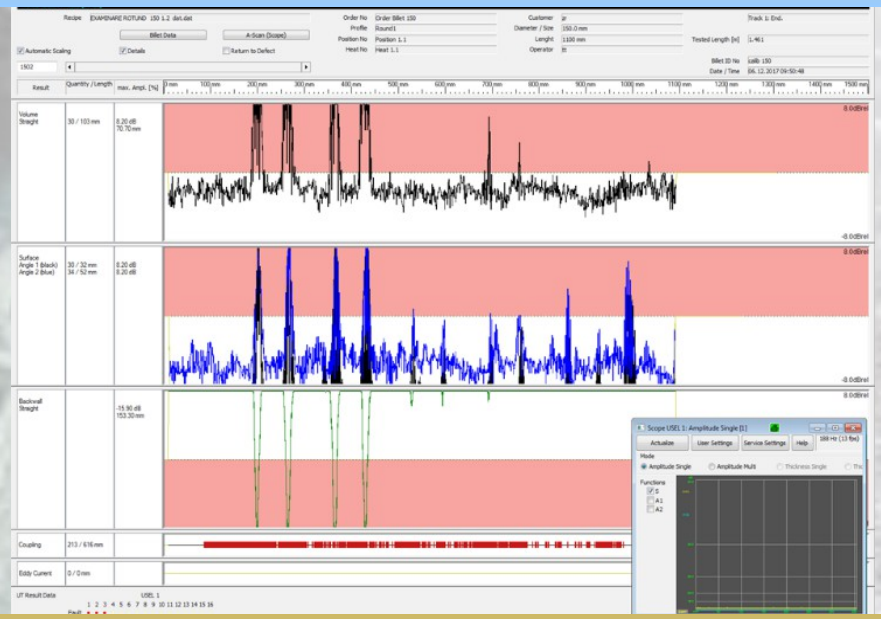

The difference between the signals of Φ 1. mm FBH and Φ 0.8 mm FBH is measured 4.7 dB instead of 7.04 dB, the theoretical value (Φ 150.0 mm reference block).

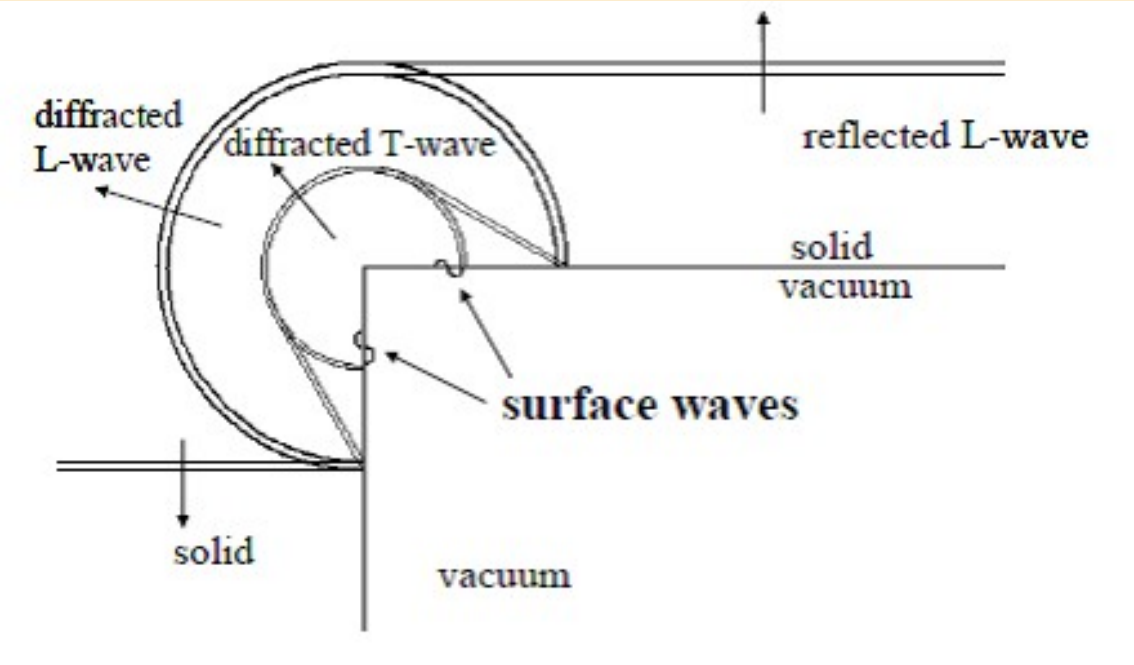

A phenomenon that the Kirchhoff approximation fails to predict is the generation of diffracted waves at the corners of the FBH

It is seen that in addition to a reflected compressional wave, diffracted compressional and shear waves are generated, along with surface waves that propagate both down the bore of the FBH and across the top.

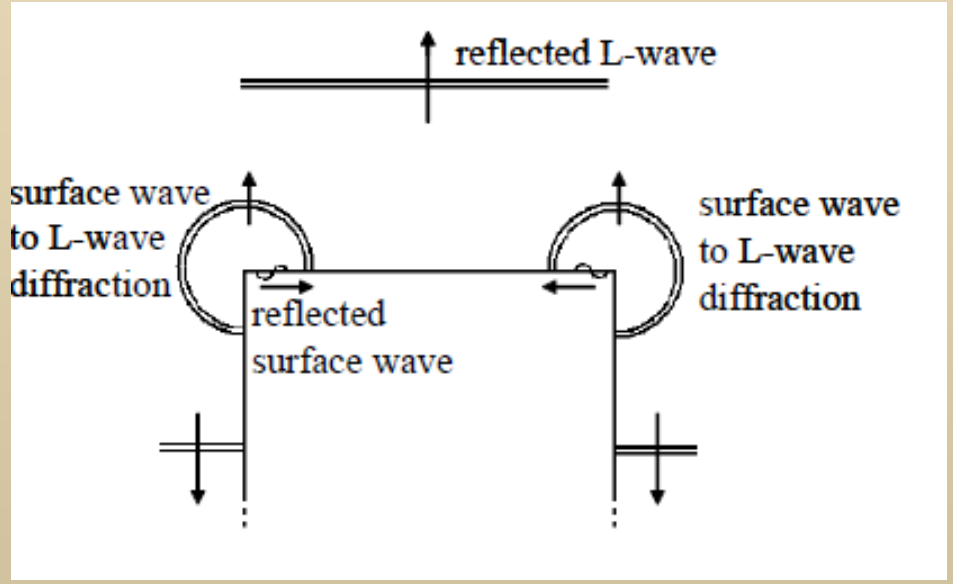

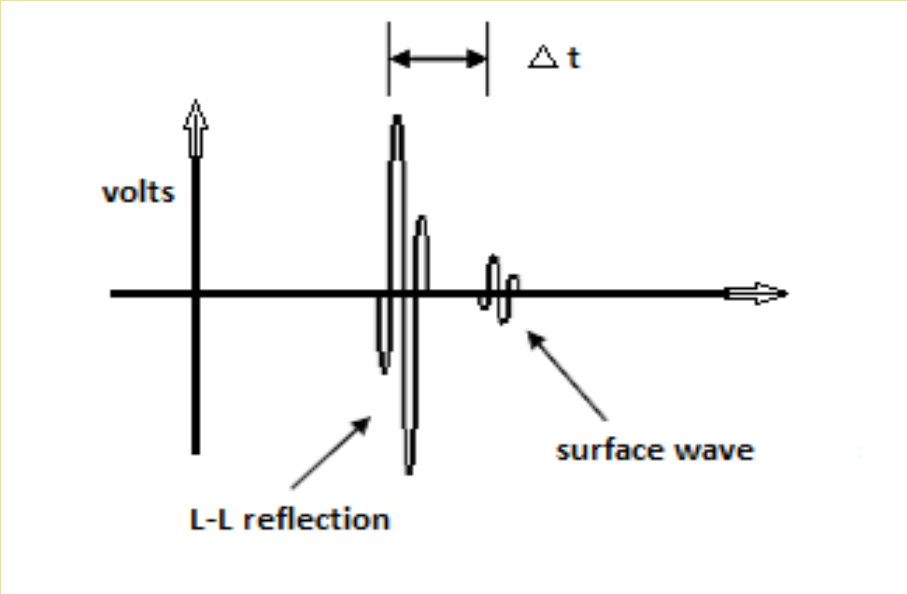

Part of this secondary diffracted wave travels up to the transducer, slightly behind the primary compressional wave reflection from the FBH surface and is received as a small signal trailing the main reflection. The time delay between these two waves is given by the product of the FBH diameter and the surface wave velocity.

If the time delay between these two signals is sufficiently small, an interaction could take place that would enhance or reduce the total signal amplitude through a constructive or destructive interference. Such an interaction might be the cause of the deviation from the area-amplitude relation seen in experiments when looking at small reflectors.

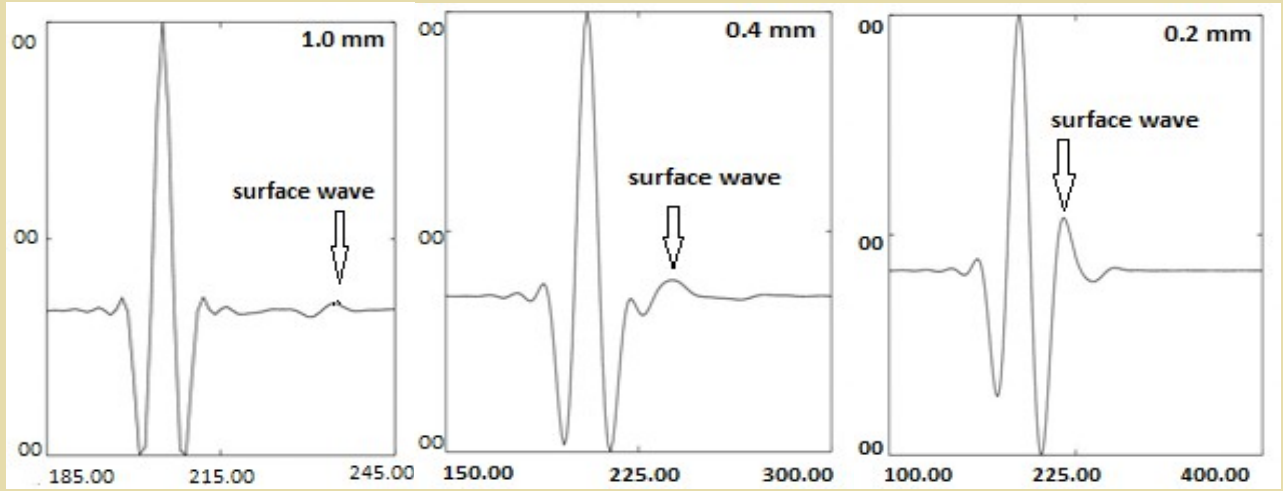

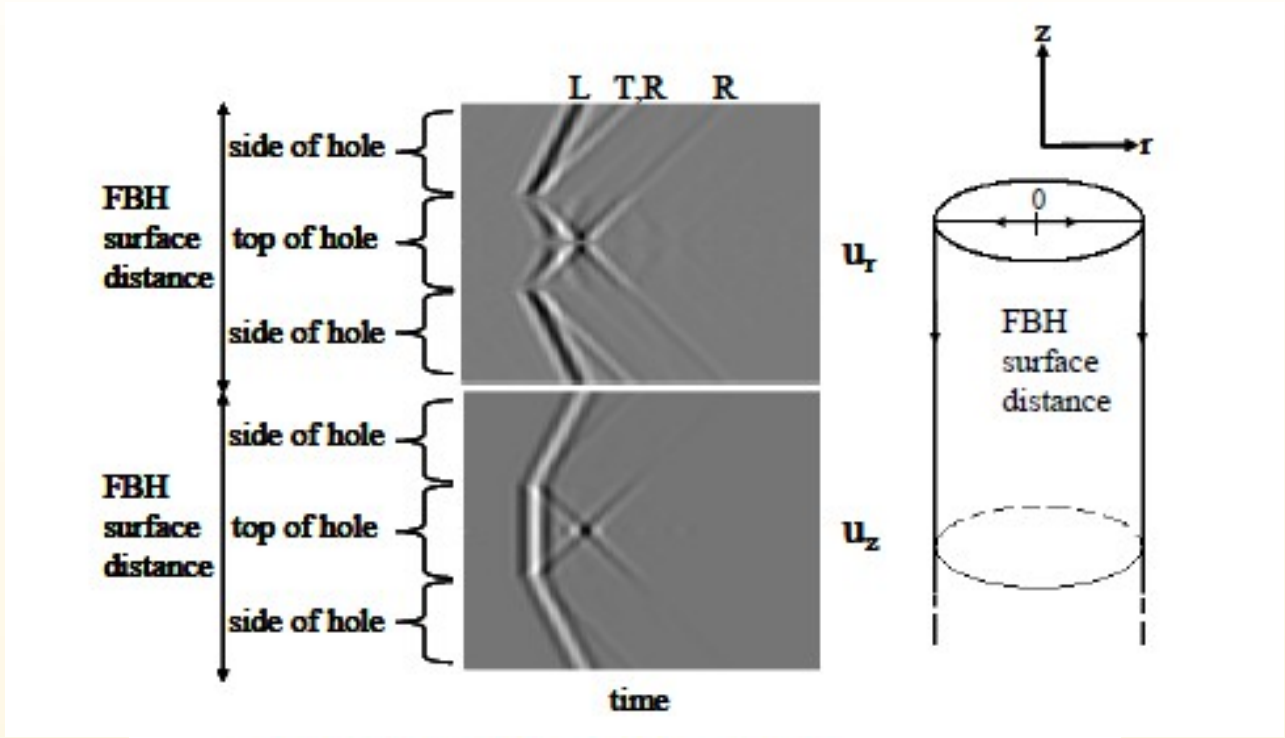

A computer model was employed that used a boundary element method (BEM) formulation to solve the equations governing the surface wave diffraction phenomena on the FBH. Image show the surface displacements in the radial and axial directions on the top and sides of the FBH as a function of time.

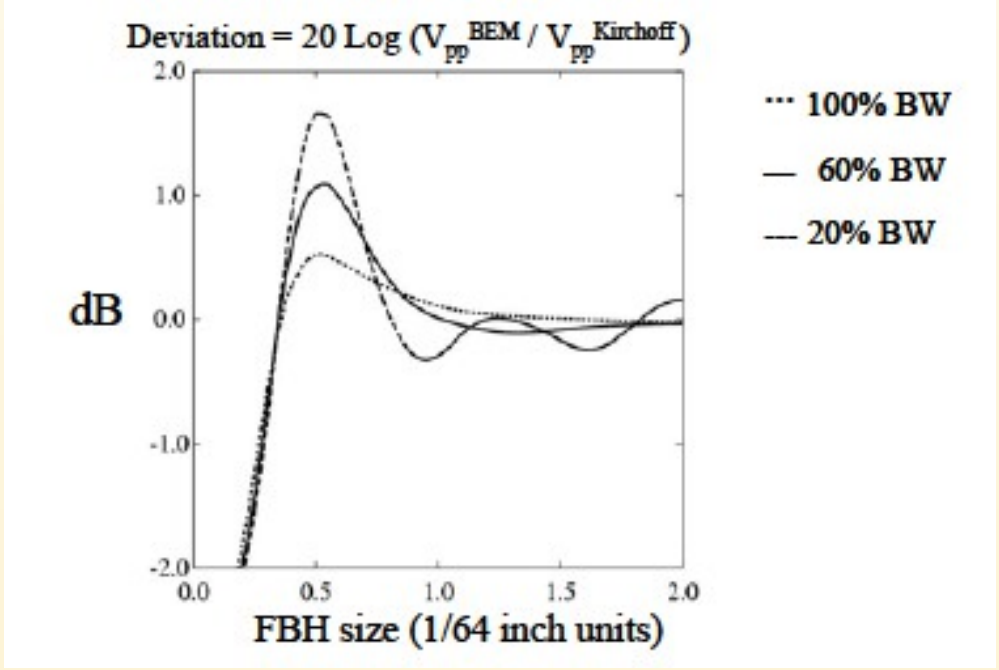

Deviation From Area-Amplitude Relationship (Kirchhoff Approximation) With Complex Signal (BEM)

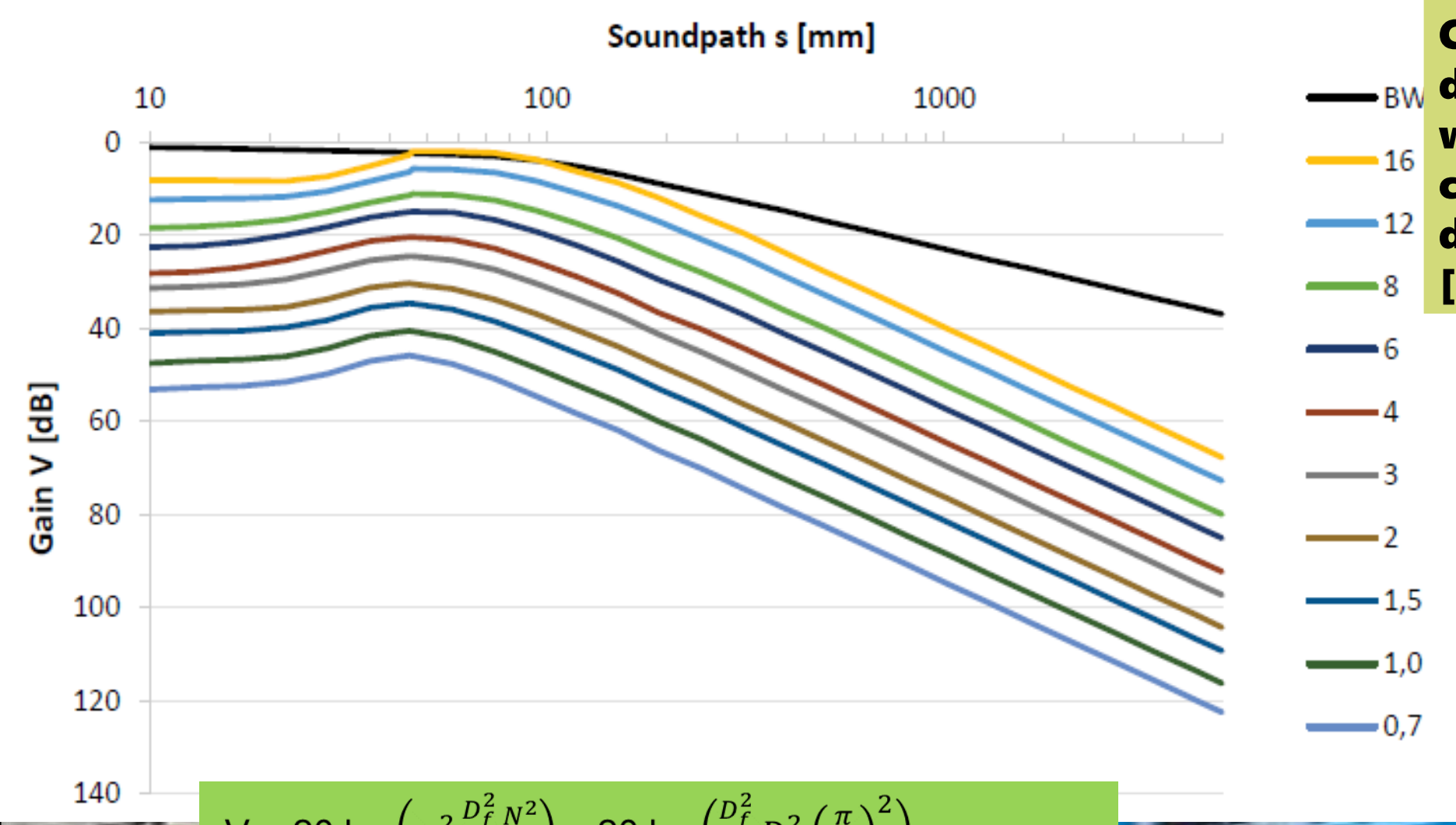

Conventional DGS diagram with the back-wall (BW) curve on top and different sizes of KSRs [mm] below

$$V = 20 \log\left(\pi^2 \frac{D_f^2}{D^2} \frac{N^2}{s^2}\right) = 20 \log\left(\frac{D_f^2}{\lambda^2} D^2 \left(\frac{\pi}{4s}\right)^2\right)$$

Df – FBH diameter,
S - Soundpath,
D- Diameter of the transducer,
N- Nearfield,
λ- the Wavelength.

The physically accurate simulation covers all physically allowed phenomena (and is not restricted by the Kirchhoff approximation).

The basic equations of linear elasto-dynamics are the conservation of momentum (Newton-Cauchy equation), the strain rate equation, and the material equations. Putting these together the wave equations in their integral form specialized for isotropic, homogenous media can be written as follows:

$$\iiint_V \underline{\underline{\underline{s}}} : \dot{\underline{\underline{T}}}(\underline{R},t)dV = \oiint_S sym\{\underline{\underline{n}}\underline{v}(\underline{R},t)\}dS + \iiint_V \underline{\underline{h}}(\underline{R},t)dV$$

$$\iiint_V \rho\dot{\underline{v}}(\underline{R},t)dV = \oiint_S \underline{\underline{T}}(\underline{R},t)\cdot\underline{dS} + \iiint_V \underline{f}(\underline{R},t)dV\ .$$

where:

T(R,t)- the symmetrical stress tensor,
v(R,t) –the particle velocity vector,
h(R,t) –the induced deformation rate tensor,
f (R,t)- induced force density vector,
s - compliance tensor,
ρ - the mass density at rest.

$$V = 20\log\left(\left[\frac{\left(i\frac{D_f}{\lambda/4}\right)^3}{\sqrt{1+\frac{1}{Q}\left(i\frac{D_f}{\lambda/4}\right)+\left(i\frac{D_f}{\lambda/4}\right)^2}}\right]\frac{1}{16}D^2\left(\frac{\pi}{4\,s}\right)^2\right)$$

Q - quality factor of the resonance effect

KSRs.

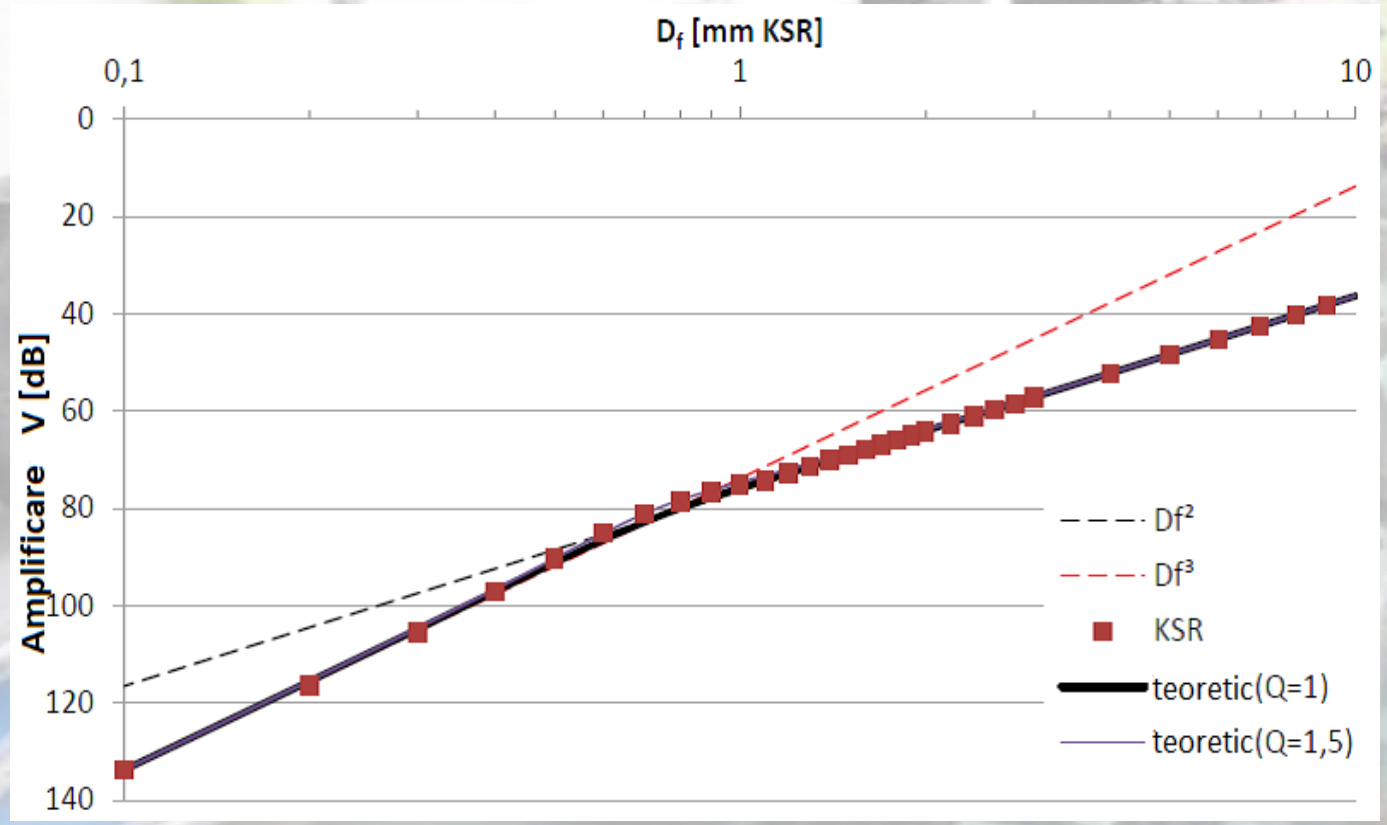

Quadratic (red dashed line) and cubic dependency on the diameter Df (black dashed line) computed gain values for KSRs (red dots); theoretical description (thick line) and equation with Q = 1,5 (thin line – slightly above the thick line).

1. Between 1,5 ($\lambda/2$) and 9 mm the simulation results follow the known DGS theory. This is the region of geometrical scattering, where the Kirchhoff approximation holds.
2. Around 0,7 mm ($\lambda/4$) the simulation results are higher. Those results are created by resonance effects and depend on the shape of the reflector.
3. For defects smaller than 0,5 mm ($\lambda/6$) the simulation results follow the cubic dependency. The cubic dependency results of Rayleigh scattering.

Simulation software for NDT

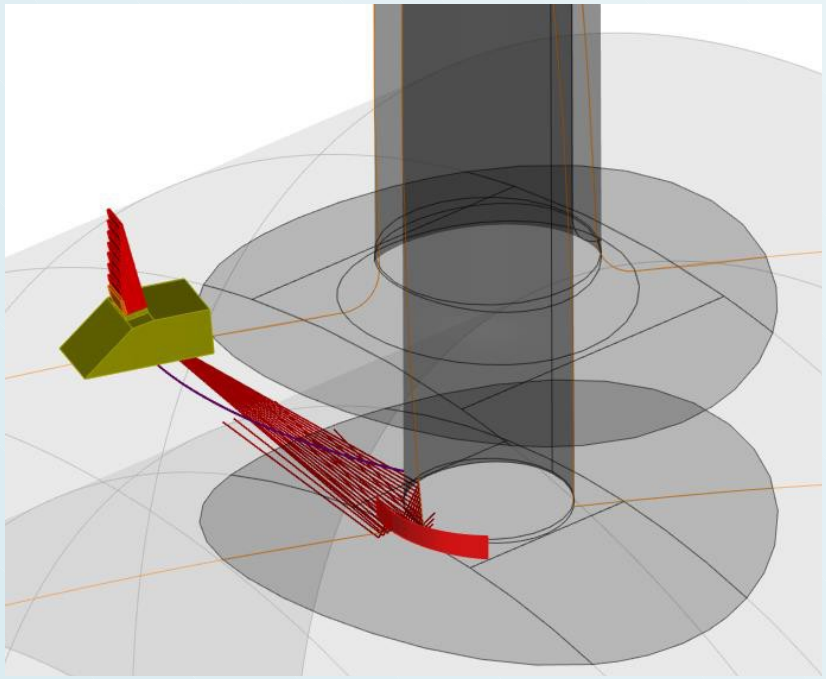

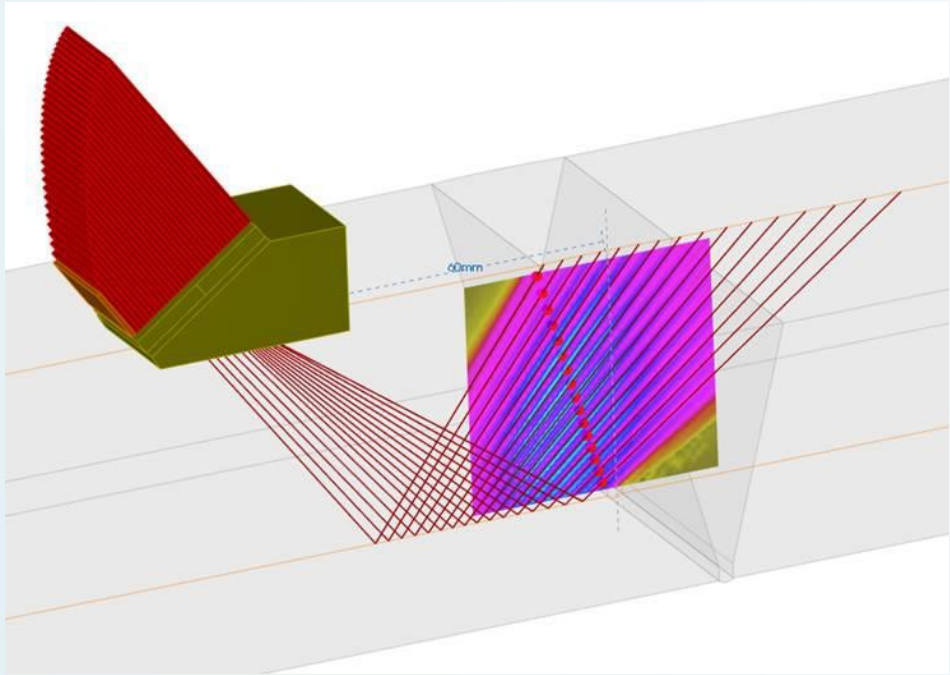

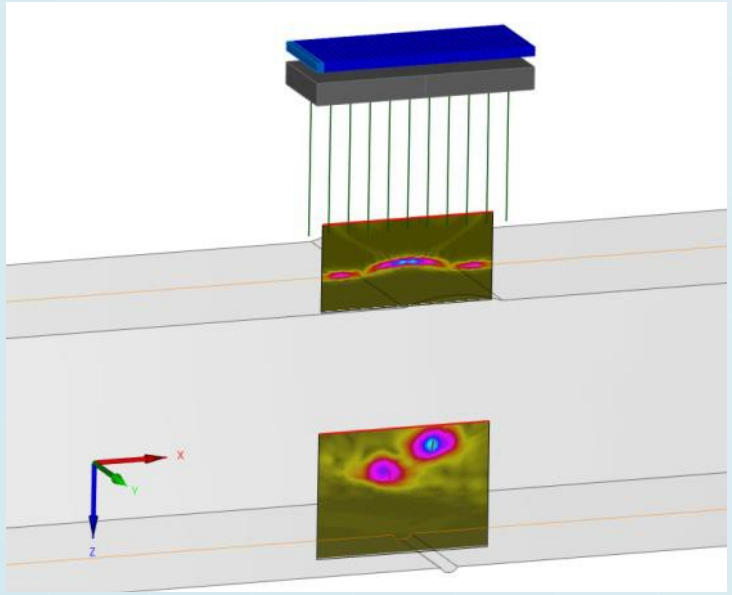

Simulation of ultrasonic Non Destructive Testing (NDT) is helpful for evaluating performances of inspection techniques and requires the modelling of waves scattered by defects. CIVA software is used more and more in connection with qualification of NDT inspection systems, both during technique development and as a part of the technical justifications.

PRINCIPLE OF THE KIRCHHOFF & GTD MODEL

- Geometrical Theory of Diffraction (GTD)
- Kirchhoff Approximation (KA)

»Kirchhoff & GTD = *Phisycal Theory of Diffraction (PTD)*

The Kirchhoff scattered field can be decomposed in an approximate manner in two parts:
a geometrical field which includes the specular reflected field and a contribution arising from the flaw edges corresponding to the edges diffraction field.

Ultrasonic field KA= Geometrical field (specular) + Diffracted field (by the defects edges)

This diffraction field contribution at the observation point x has the same form as the GTD field but a different edge diffraction coefficient (depending on the α incidence and β observation directions and polarizations).

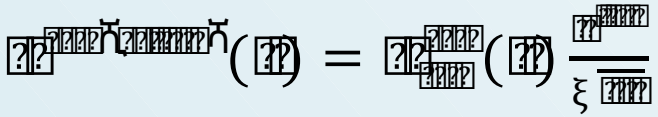

The physical theory of diffraction (PTD) consists in correcting the Kirchhoff edge diffraction field by that modelled by GTD. This correction leads to add a corrective term to the KA scattered field (without far-field approximation). This corrective term is the difference of wave amplitudes diffracted by the edge given by GTD and KA.

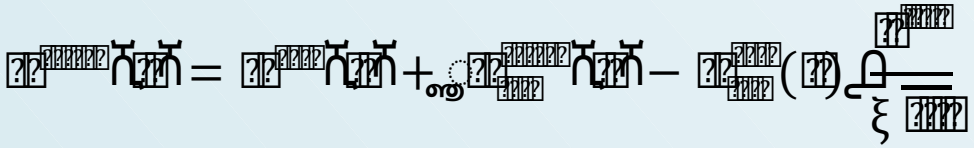

But the KA diffraction coefficient KA, $D^{KA}_{\alpha\beta}(x)$ for edge diffraction contribution (previously obtained from a far field approximation of the Kirchhoff field) diverges and has the same singularity as the GTD edge diffraction coefficient GTD, $D^{GTD}_{\alpha\beta}(x)$. When making the difference of the two coefficients, their singularities cancel each other and the diffraction coefficients difference $D^{GTD}_{\alpha\beta}(x) - D^{KA}_{\alpha\beta}(x)$ is finite.

$$U^{PTD}(x) \approx U^{KA}(x)$$

When the observation direction is far from to the specular direction, edge diffraction effects are predominant compared to reflection phenomena, the Kirchhoff field is equal to the Kirchhoff edge diffraction contribution and so cancels it so that the Kirchhoff & GTD model leads to similar results than the GTD model.

$$U^{KA}(x) \approx D^{KA}_{\alpha\beta}(x)\frac{e^{ikr}}{\sqrt{kr}} \text{ and } U^{PTD}(x) \approx D^{GTD}_{\alpha\beta}(x)\frac{e^{ikr}}{\sqrt{kr}} = U^{GTD}(x)$$

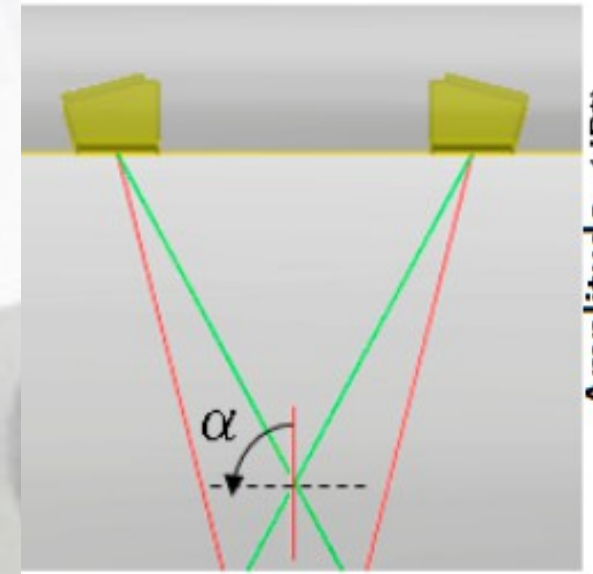

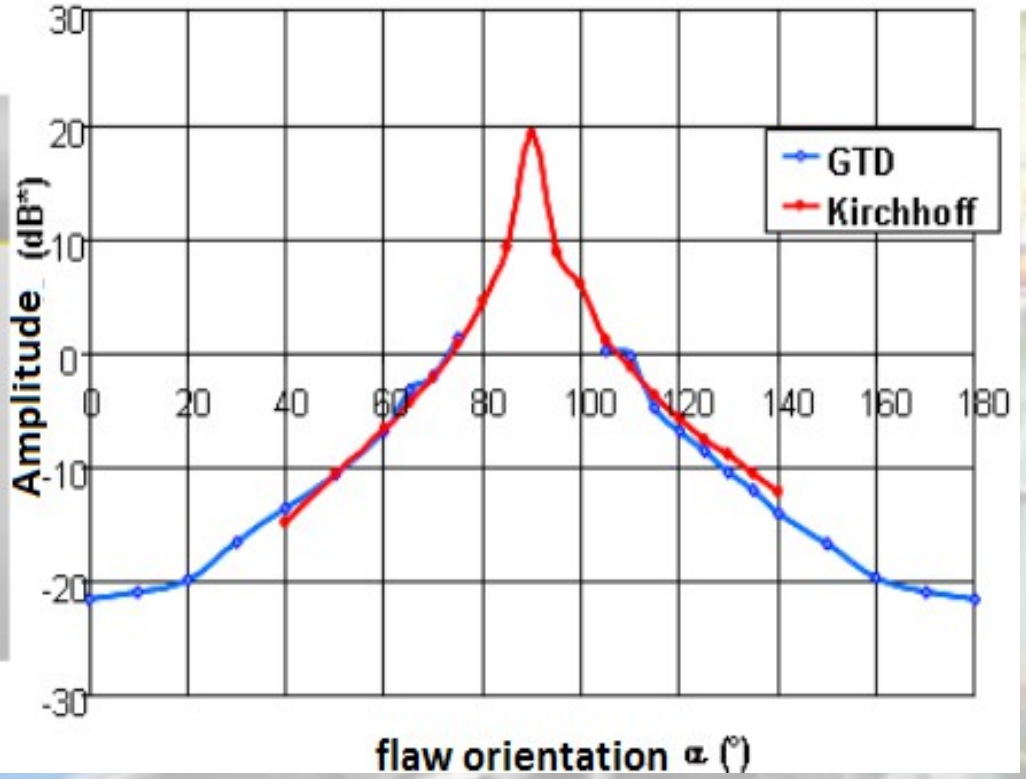

Applicability of Kirchhoff and GTD models

SV45 pulse echo configuration.
a) Orientation of the crack (thick black line) is specified by the angle,
b) Maximum displacements calculated using GTD (blue line), Kirchhoff approximation (red line) and corrected Kirchhoff approximation (green line).

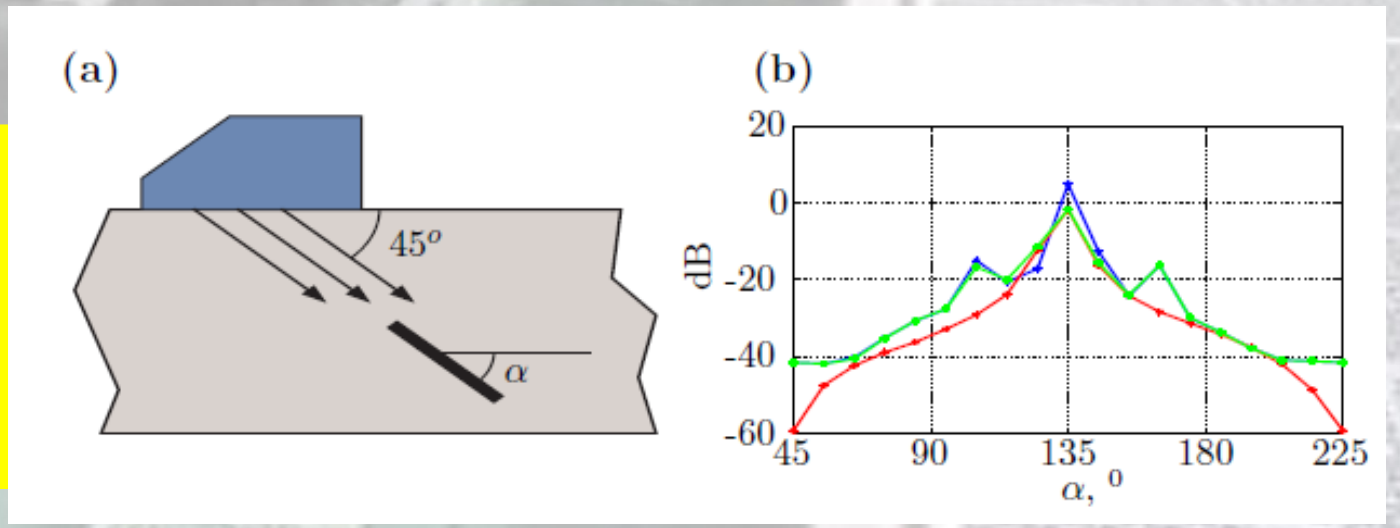

Model capability to be assessed

- Wavelength of the ultrasonic field has to be small when compared with some characteristic length of the model. Failure to comply can make the calculation unreliable.
-Kirchhoff's approximation is a high frequency approximation, valid when the defect is greater than the wavelength, that is, when ka >>1, where k is the wavenumber and a is the main dimension of the defect.

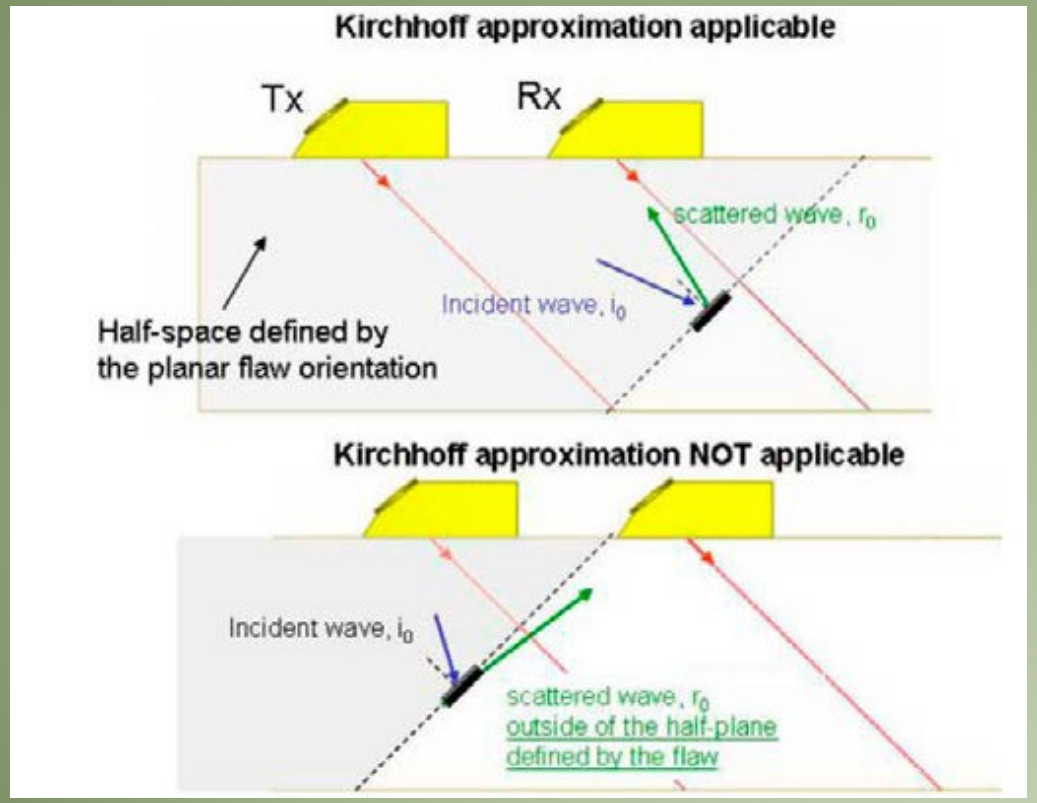

For the first position (top of the figure), both probes are lying on the same side of the flaw, an echo is calculated. For the second position (bottom of the figure), the axis of the receiving probe doesn't lie in the half space defined by the flaw orientation, therefore one cannot predict the echo scattered by the flaw because the Kirchhoff developed model is not applicable (the receiving probe is lying in the so-called' shadowed area'). "

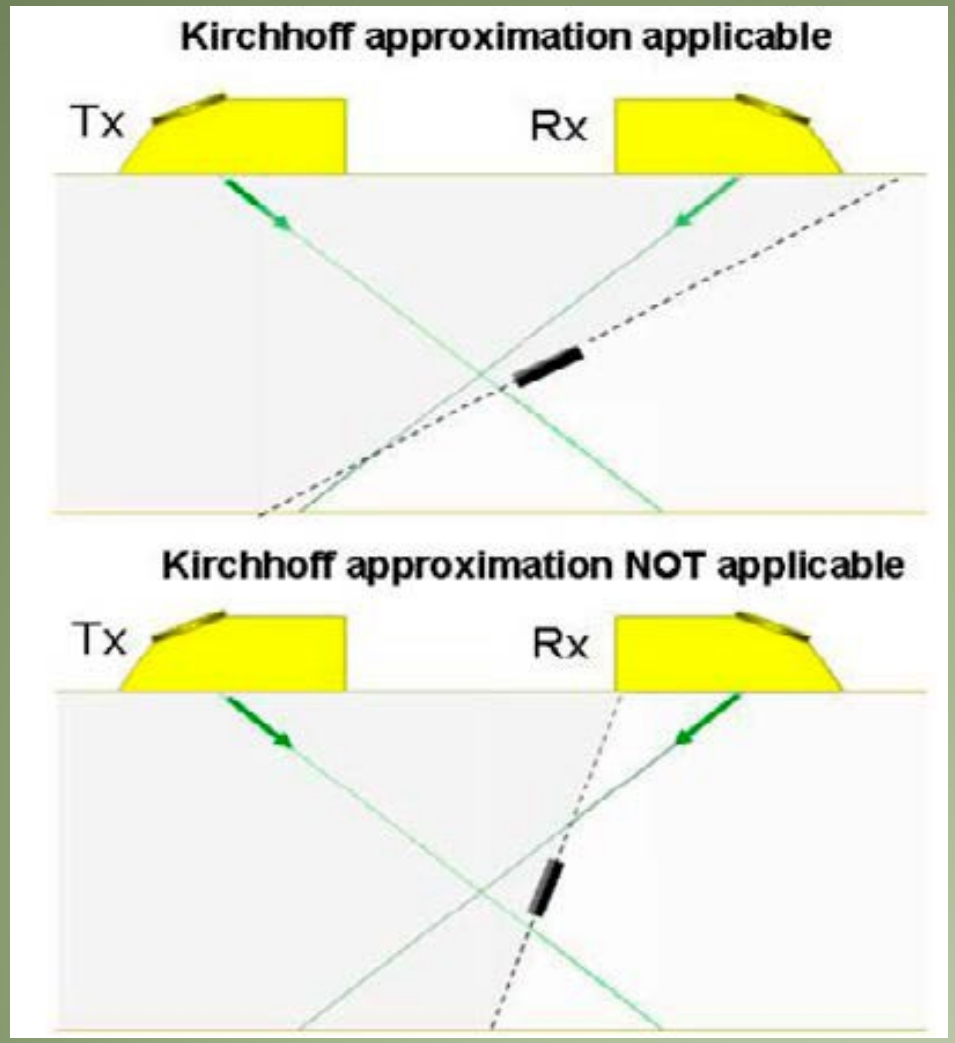

Similar limitations occur when using a pair of probes in TOFD inspection (see following figure) for nearly vertical flaws: The Kirchhoff model will soon be not applicable as the orientation of the flaw prevents the axis of the transmitter and receiver probes lying from the same side of the flaw. On the following figure, only the configuration displayed on top can be simulated using the Kirchhoff model.

Tip diffraction echoes from planar defects can be accurately predicted using the Kirchhoff approximation in terms of time of flight, however their amplitudes cannot be quantitatively predicted using the Kirchhoff model. The quantitative error is expected to increase when the scattered direction moves away from the specular direction.

Applications in the Ultrasonic Standards Evaluation

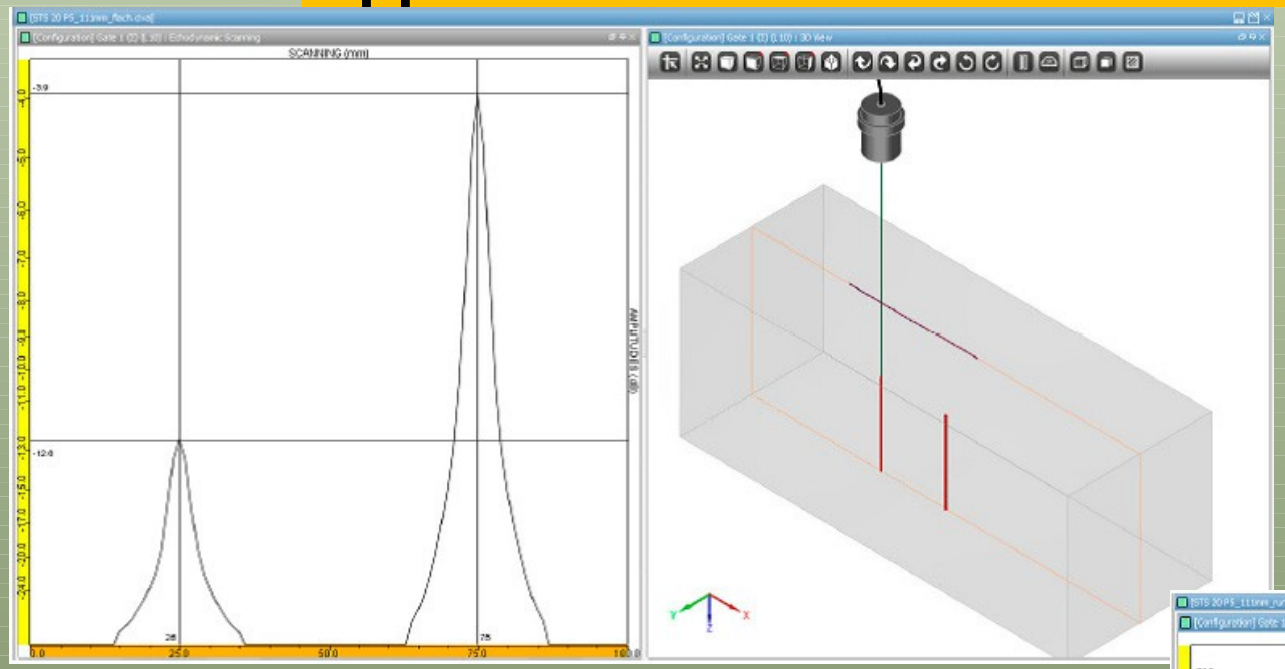

- Flat faced reference block, 111 x 111 mm square dimensions,
- Round reference block, 111 mm diameter,
- Round reference block, 265 mm diameter.

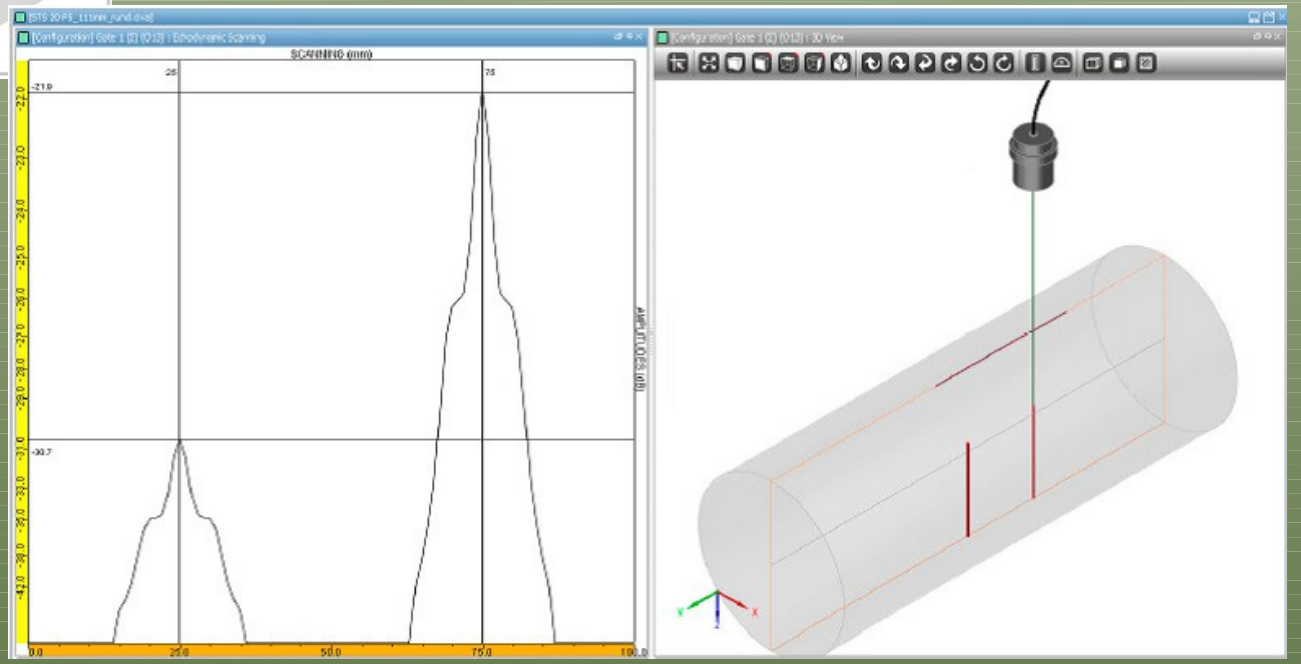

All holes are positioned with the reflecting surface at 50 mm depth in the material.

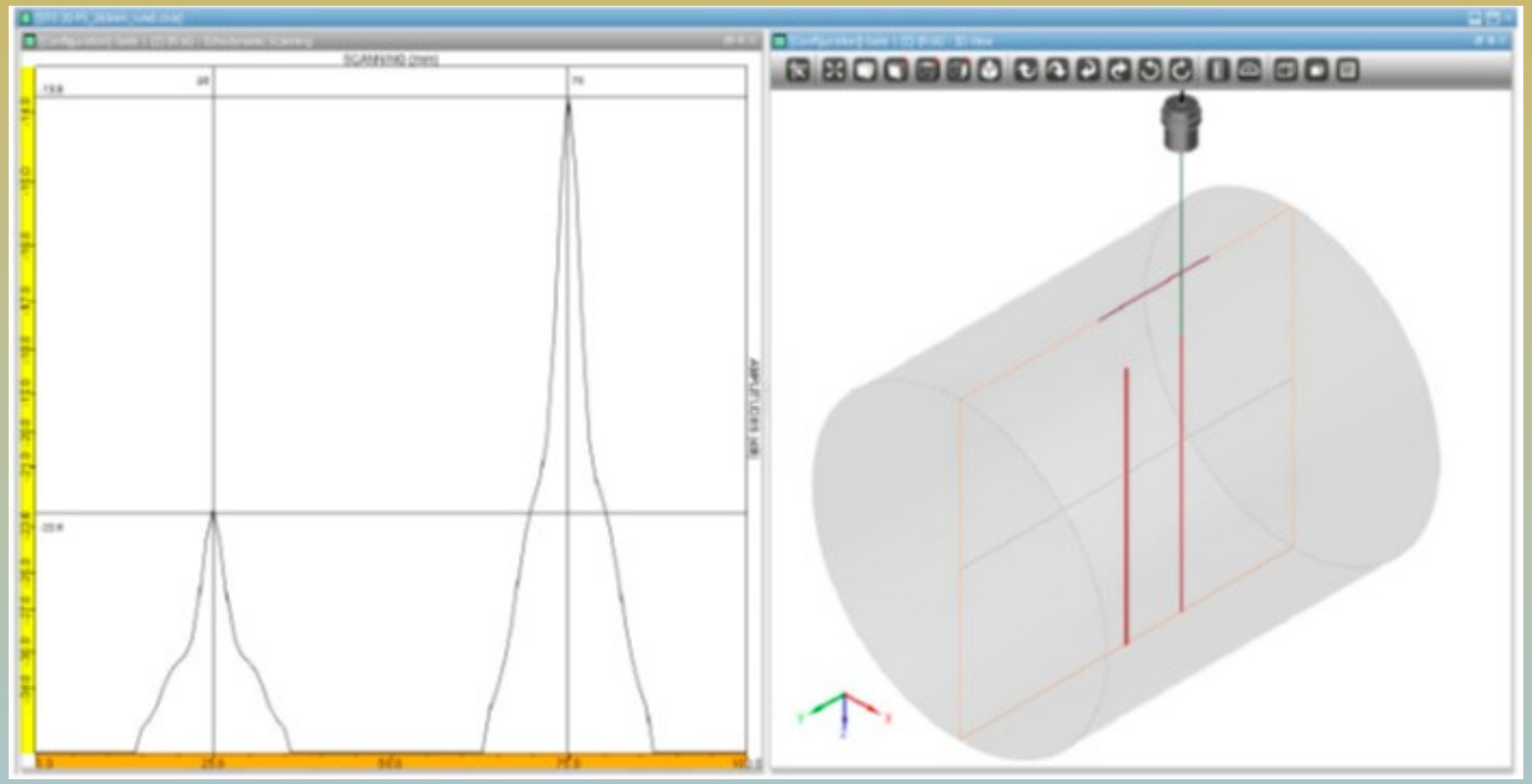

Each reference block is provided with one pair of FBH having the diameters of Φ1,2 and Φ 2.0 mm, first determination - Table 1, and Φ 0.8 mm and Φ1.2 mm, second determination-Table 2.

STS 20 P5 – imersion transducer, non focused, 20 mm crystal diameter, 5MHz central frequency.

STS 20 P5 L125 – imersion transducer, 125 mm focal distance in water, 20 mm crystal diameter, 5MHz central frequency.

STS 20 P5 L200 - imersion transducer, 200 mm focal distance in water, 20 mm crystal diameter, 5MHz central frequency.

Test specimen	Test flaw	STS 20 P5		STS 20 P5 L125		STS 20 P5 L200	
billet 111x111 mm	FBH Ø 1.2 mm	-12.6 dB	Δ=8.7 dB	-9.4 dB	Δ=8.7 dB	-8.6 dB	Δ=8.6 dB
	FBH Ø 2.0 mm	-3.9 dB		-0.7 dB		0 dB	
Bar Ø 111 mm	FBH Ø 1.2 mm	-30.7 dB	Δ=8.8 dB	-16.8 dB	Δ=8.8 dB	-21.3 dB	Δ=8.7 dB
	FBH Ø 2.0 mm	-21.9 dB		-8 dB		-12.6 dB	
Bar Ø 265 mm	FBH Ø 1.2 mm	-22.6 dB	Δ=8.8 dB	-11.6 dB	Δ=8.7 dB	-14.1 dB	Δ=8.7 dB
	FBH Ø 2.0 mm	-13.8 dB		-2.9 dB		-5.4 dB	

Table 1

For the FBH pair of Φ 1.2 - Φ 2.0 mm, the amplitude differences obtained with CIVA 11 are in the range of 8.6÷8.8 dB, very close of the theoretical value of 8.87 dB (see Table 1). Similarly for the FBH pair of Φ 0.8-Φ 1.2 mm, where the difference determined by the program CIVA 11 are in the range of 6.8÷7.0 dB and the calculated value is 7.04 dB (see Table 1).

Sound path in water is set 100 mm for all determinations. Sound speed in material and specific attenuation are identical for all determinations.

Test specimen	Test flaw	TS 20 WB4		STS 20 P5 L125		STS 20 P5 L200	
billet 111x111 mm	FBH Ø 0.8 mm	-7.2 dB	Δ= 7 dB	-7.7 dB	Δ= 7 dB	-6.9 dB	Δ= 6.9 dB
	FBH Ø 1.2 mm	-0.2 dB		-0.7 dB		0 dB	
Bar Ø 111 mm	FBH Ø 0.8 mm	-21.9 dB	Δ= 7 dB	-15.2 dB	Δ= 7 dB	-19.7 dB	Δ= 7 dB
	FBH Ø 1.2 mm	-14.9 dB		-8.2 dB		-12.7 dB	
Bar Ø 265 mm	FBH Ø 0.8 mm	-14.5 dB	Δ= 6.8 dB	-9.9 dB	Δ= 6.9 dB	-12.3 dB	Δ= 6.8 dB
	FBH Ø 1.2 mm	-7.7 dB		-3 dB		-5.5 dB	

Similarly for the FBH pair of Φ 0.8-Φ 1.2 mm, where the difference determined by the program are in the range of 6.8÷7.0 dB and the calculated value is 7.04 dB (see Table 2).

Table 2

The resulting values (noted with Δ in Table 1 and Table 2) match the theoretical values obtained for the proportion of the surfaces of the artificial defects. For defects smaller than the wavelength, it was proven in reality that the differences between the two holes are different that these values.
As observed, these differences are more pronounced as the product ka >>1 (*k* = wave number and *a* = size of the artificial defect).

These experiments prove the limitations of the CIVA 11 simulation software for the defects close to the specular area and geometrical reflex whereas the software applies the Kirchhoff Approximation and does not consider the diffraction phenomenon that appear at the edge of FBH.

OPTIMIZATION OF THE ULTRASONIC INSPECTION

The transducer with the best ultrasonic behavior can be decided by comparing the observed amplification reserve with the value initially selected for each of the 3 transducers. For an example, if Table 1, row 1 - billet 111x111 mm and Table 1, row 2 - BAR Φ111 mm are selected:

Row 1, FBH Φ 1.2 mm represents the inspection of a defect located at a depth of 50 mm below the entry plane surface. The best result is provided by the transducer STS 20 P5 L 200 (-8,6 dB) due to optimal Pulse Volume for a defect located at a 50 mm depth related to its focal distance in water.

Row 1, FBH Φ 1.2 mm represents the inspection of a defect located at a depth of 50 mm below the entry plane surface. The best result is provided by the transducer STS 20 P5 L 200
(-8,6 dB) due to optimal Pulse Volume for a defect located at a 50 mm depth related to its focal distance in water

Test specimen	Test flaw	STS 20 P5		STS 20 P5 L125		STS 20 P5 L200	
billet 111x111 mm	FBH Ø 1.2 mm	-12.6 dB	Δ=8.7 dB	-9.4 dB	Δ=8.7 dB	-8.6 dB	Δ=8.6 dB
	FBH Ø 2.0 mm	-3.9 dB		-0.7 dB		0 dB	
Bar Ø 111 mm	FBH Ø 1.2 mm	-30.7 dB	Δ=8.8 dB	-16.8 dB	Δ=8.8 dB	-21.3 dB	Δ=8.7 dB
	FBH Ø 2.0 mm	-21.9 dB		-8 dB		-12.6 dB	
Bar Ø 265 mm	FBH Ø 1.2 mm	-22.6 dB	Δ=8.8 dB	-11.6 dB	Δ=8.7 dB	-14.1 dB	Δ=8.7 dB
	FBH Ø 2.0 mm	-13.8 dB		-2.9 dB		-5.4 dB	

The most efficient transducer is STS 20 P5 L 125 with a focal length in water of 125 mm. Due to the radius of the entry surface, the focal distance in the material is increased and this transducer presents now the focal distance in the area of depth of the artificial defect (50mm). The gain difference is increased significantly comparing with the other 2 transducers: 4.5 dB versus the transducer focalized with the focal distance of 125 mm and 13.9 dB versus the unfocalized transducer. This is caused by the defocusing of the immersion transducers at incidence of the ultrasonic beam with the cylindrical surface of the billet and due to the modification of the Pulse Volume in the area of the targeted defect.

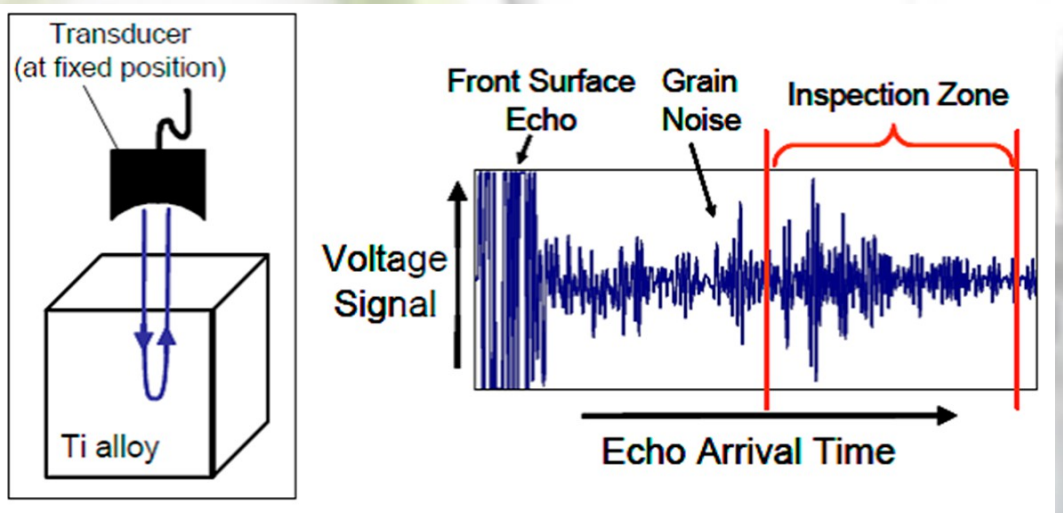

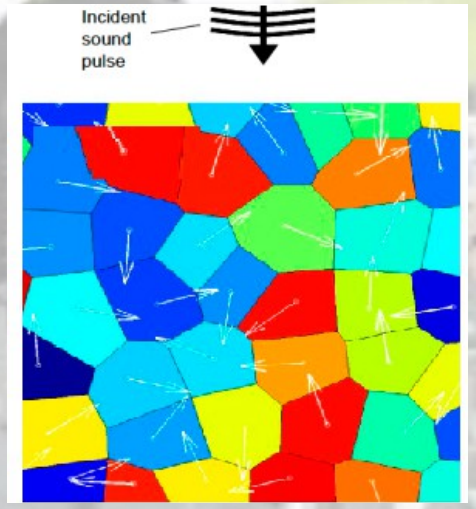

CONCLUSION

Unfortunately, the largest discrepancy between the software simulations and experiments is noise, or rather signal to noise ratio. Defects responses are often evaluated in relation to the surrounding noise levels rather than an arbitrary reference target, such as a notch or SDH.

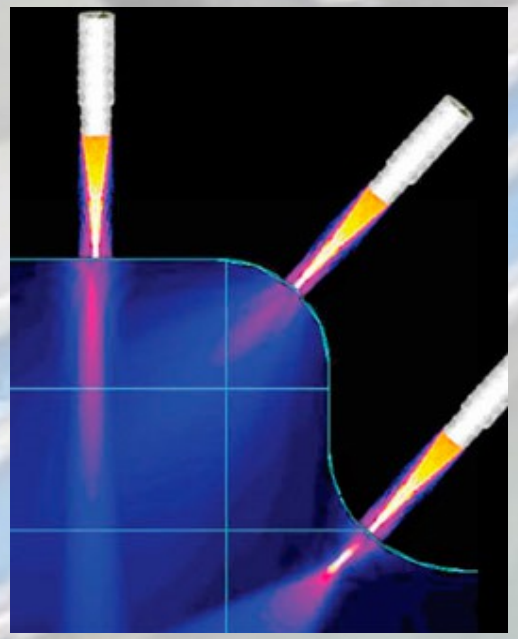

It is not possible to simulate a complete inspection, or validate an inspection procedure by simulations with CIVA at the current time. The conclusion is that simulations using CIVA can be used when specific problems or technical solutions must be solved or developed, e.g. the influence of the surface curvature over the Pulse Volume or the correct choice of the inspection configuration.

The inspection's optimization is achieved today both by minimizing the noise of the material and by adopting the inspection techniques capable to highlight and perform a correct evaluation of the discontinuities smaller than one wavelength, according to the highest quality standards.

THANK YOU!